Linear response of east Greenland's tidewater glaciers to ocean/atmosphere warming

Supporting Information

T. Cowton[1], A. Sole[2], P. Nienow[3], D. Slater[4], and P. Christoffersen[5]

[1]School of Geography and Sustainable Development, University of St Andrews, KY16 9AL, UK
[2]Department of Geography, University of Sheffield, S10 2TN, UK
[3]School of Geosciences, University of Edinburgh, EH8 9XP, UK
[4]Scripps Institute of Oceanography, UC San Diego, La Jolla, CA 92093, USA
[5]Scott Polar Research Institute, University of Cambridge, CB2 1ER, UK

Introduction

This supplement contains a detailed description of the methods employed in this study, as well as additional tables and figures referenced directly from the main text.

Methods

Study glaciers

Details of the 10 study glaciers are given in Table S1. These glaciers represent a subset of the 32 glaciers documented by Seale *et al* (2011), chosen to span a range of conditions along the east coast of Greenland. Within each region, the largest outlet glaciers (with respect to ice velocity and terminus width; Table S1) were selected. In the far northeast of Greenland, the major outlet glaciers drain into substantial floating ice tongues (e.g. Wilson et al., 2017). Charting the retreat of these glaciers (where changes in grounding line position rather than calving front position are likely of primary importance) is not possible with the methods employed here, and so no glaciers were selected in this region.

Air temperature

Mean summer air temperature (Figure 2a-b), T_A, is based on the May-September mean of monthly temperatures from ERA-Interim global atmospheric reanalysis (Dee et al., 2011). For each glacier, temperatures are extracted from the reanalysis cell in which the terminus lies. To account for differing mean topography between cells, these values are adjusted to give sea level temperature assuming an atmospheric lapse rate of 0.0065 °C / m.

Abbrevi-ation	Glacier	Latitude, Longitude	Terminus width (km)	Ice velocity (m yr^{-1})
Southern glaciers				
M3	Mogens 3	62.52, -43.04	1.7	2140
T1	Tingmjarmiut 1	62.76, -43.21	3.1	3980
AB	AP Bernstorffs Glacier	63.82, -41.69	4.7	2450
HG	Helheim Glacier	66.35, -38.18	7.3	6500
KG	Kangerdlugssuaq Glacier	68.59, -32.86	6.6	5130
Northern glaciers				
BG	Borggraven	68.60, -28.05	4.7	920
VG	Vestfjord Glacier	70.38, -29.09	3.5	2060
DJ	Daugaard-Jensen Glacier	71.90, -28.59	4.0	3330
WG	Waltershausen Glacier	73.83, -24.30	11.9	100
HK	Heinkel Glacier	75.16, -22.46	3.0	70

Table S1. Details of the ten study glaciers in east Greenland. Velocities are averaged along the lowermost 5 km of each glacier, and are taken from the MEaSUREs Greenland ice sheet velocity map (Joughin et al., 2010a, Joughin et al., 2010b) for the year 2000-2001 in all cases except BG and WG, which due to restricted coverage are from the equivalent map for the year 2005-2006.

Runoff

Annual mean catchment runoff, Q, for each of the 10 glaciers (Figure 2c-d) is obtained from a 1 km surface melting, retention and runoff model forced with ERA-Interim reanalysis (Wilton et al., 2017). Runoff due to basal melting is expected to be limited and is therefore not considered. Meltwater is routed through glacial catchments using the hydraulic potential gradient (Shreve, 1972) based on the ice surface and bed topography (Bamber et al., 2013). Q is predicted to be greatest at KG due to its large catchment area and more melt-favourable hypsometry relative to HG and DJ, which have comparable catchment areas (Figures 1 and 2c-d).

Ocean temperature

We seek to compare changes in glacier terminus position to a measure of ocean water temperature, T_O, in the fjords adjacent to the glaciers. Because there are few *in situ* hydrographic measurements from fjords, and the fjords are not well resolved in ocean circulation models, we define $T_O = T_R + c$, where T_R is ocean temperature based on reanalysis values for the continental shelf and c is a correction to account for temperature differences between the shelf and fjords.

T_R is obtained from the GLORYS2V3 1/4° ocean reanalysis product (Ferry et al., 2012). A decision must be made as to where to sample these data for each glacier. Because cross-shelf troughs are

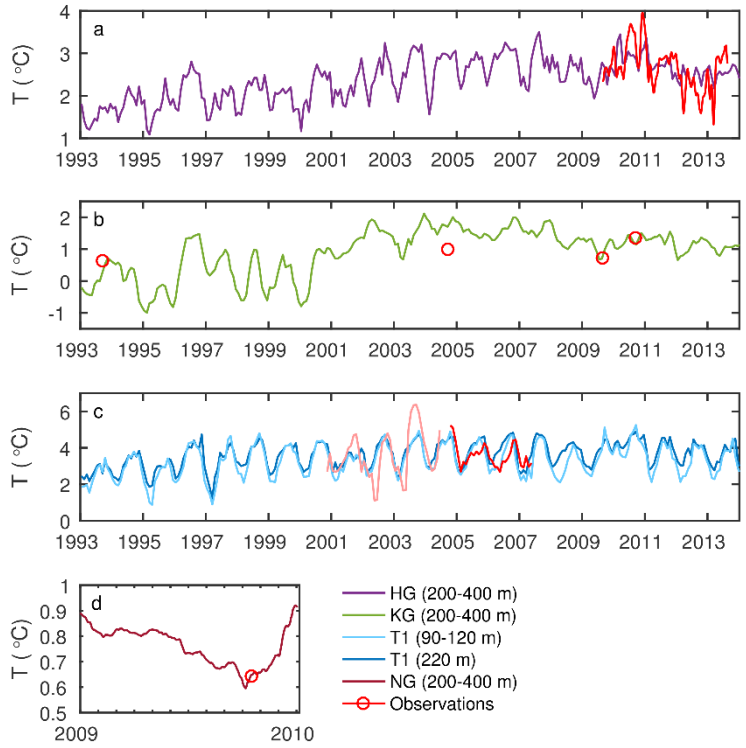

Figure S1. Comparison of ocean temperature T from reanalysis (as for Figure 2c-d) and *in situ* observations at (a) HG (Straneo et al., 2016) (b) KG (Azetsu-Scott and Syvitski, 1999, Dowdeswell, 2004, Straneo et al., 2012, Inall et al., 2014a) (c) T1 (Murray et al., 2010) and (d) Nioghalvfjerdsbræ (NG) (Wilson and Straneo, 2015). For *in situ* data, continuous lines and circles show data from moorings and CTD surveys respectively. (a), (b) and (d) show depth-average temperatures from 200-400 m. For (c), the *in situ* record switches from 90-120 m (pink) to ~220 m (red) depth in summer 2004, and so both depths are plotted for the corresponding reanalysis data (light blue and dark blue respectively). Otherwise, colours for reanalysis data are as for Figures 1 and 2, with *in situ* observations overlaid in red. The plotted reanalysis time series have been adjusted to fit *in situ* observations by subtracting constant values of (a) 2.9 °C, (b) 3.1 °C, (c) 1.5 °C and (d) 0.3 °C.

poorly mapped and not well resolved in the reanalysis, cells close to fjord mouths tend to be unrealistically shallow (e.g. Fenty et al., 2016) and so the warmer, deeper waters (crucial to the fjord heat budget) are not captured. Conversely, if the nearest cell of depth equal to that of the grounding line is chosen, this can be hundreds of kilometres away from the fjord mouth on the shelf break, and it is not clear that a pathway of such depth will exist between that cell and the glacier. As a compromise, we opt for the nearest cell of depth > 400 m, which is deep enough to sample the warmer Atlantic waters (AW) existing at depths greater than ~ 200 m whilst in many cases being located on the shelf rather than beyond the shelf break (Figure 1). For simplicity and consistency between glaciers, we take T_R as the annual mean temperature between 200-400 m (Figure 2e-f). This falls within the likely depth range of up-fjord currents (e.g. Cowton et al., 2016), and allows key inter-annual trends in AW temperature to be captured whilst reducing noise due

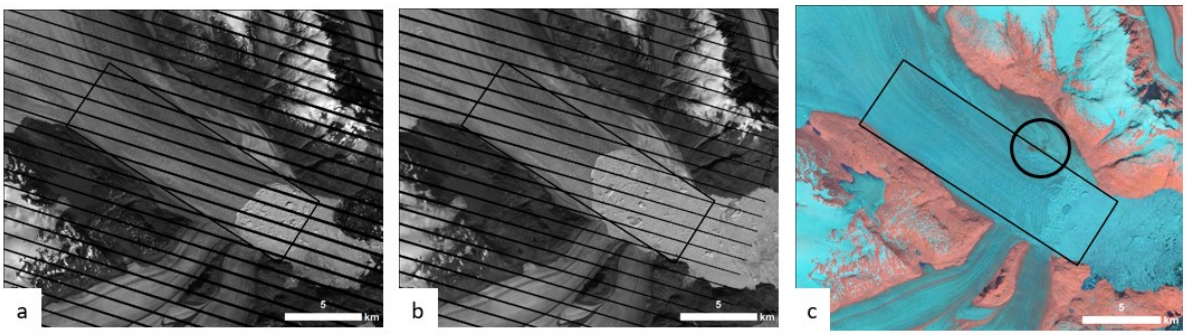

Figure S2. (a-b) Landsat 7 images of KG acquired on (a) 21 August 2004 and (b) 15 August 2005, documenting the rapid retreat of the terminus over this time. A bedrock high (c, black circle), marking the position of the 2005 pinning point, is visible in a Landsat 8 image acquired on 18 July 2016.

to large seasonal variations in shelf surface water temperatures which likely have limited influence on the glaciers (Straneo and Heimbach, 2013).

To obtain values for the correction term *c,* we test these time series of T_R against available *in situ* observations from moorings and CTD surveys in the vicinity of T1 (Holfort et al., 2008, Murray et al., 2010), HG (Straneo et al., 2016), KG (Azetsu-Scott and Syvitski, 1999, Dowdeswell, 2004, Straneo et al., 2012, Inall et al., 2014b) and, in the absence of data from the northern study glaciers, Nioghalvfjerdsbræ (NG) in the far north east of Greenland (Wilson and Straneo, 2015) (Figures 1 and S1). Fitting of T_R to the observations indicates that the reanalysis data overestimate *in situ* temperatures in these locations by approximately 1.5 °C (T1), 2.9 °C (HG), 3.1 °C (KG) and 0.3 °C (NG). While this may in part reflect errors in the reanalysis product (which is poorly constrained by observations on the shelf), significant cooling of AW is expected as it crosses the continental shelf from the core of the warm currents at the shelf break to the fjords (Straneo et al., 2012). To better represent the temperature of subsurface waters entering the fjords, we use these observations to adjust the values of T_R derived from the reanalysis data to give T_0. For the cluster of glaciers in southeast Greenland (M3, T1 and AB) we set c = 1.5 °C, while at HG and KG we set c = 2.9 °C and 3.1 °C respectively. For the glaciers in northeast Greenland (BG, VG, DJ, WG, HK), influenced by the same cooler recirculated AW as NG (Straneo et al., 2012), we set c = 0.3 °C. These offsets are then used to calculate the values of T_0 used throughout the paper. While this adjustment is necessarily approximate given the scarcity of *in situ* observations, its application enables better representation of the temporal and spatial variability in the temperature of ocean water entering Greenland's fjords.

Terminus position

For the period 2000-2009, width-averaged changes in glacier terminus position P (expressed as distance from an arbitrary up-glacier location) are taken from Seale *et al* (2011) and based on the automated classification of all available MODIS imagery. We extend this time series by manual termini delineation (using the linear box method (Lea et al., 2014)) in Landsat scenes (e.g. Figure S2) at approximately monthly intervals over the period 2009-2015, and where available over the period 1990-1999. No Landsat scenes are available during the years 1991, 1993 and 1995. At KG, HG and DJ we supplement these data with terminus positions delimited using Envisat imagery by Bevan *et al* (2012).

Because the glaciers typically undergo an annual cycle of advance and retreat, error will be introduced into the mean annual position for glaciers and years where there are significant gaps in the available coverage. We therefore adjust glacier lengths according to

$$P = P_{mean} + \left(\frac{1}{2}\mu_a r\right), \tag{S1}$$

where P is the adjusted mean annual terminus position, as based on P_{mean}, which is the mean of the available data for each year. r is the typical annual range in terminus positions for each glacier, based on the period 2010-2013 when continuous Landsat availability gives accurate near year-round coverage (Table S2). Each data point is given a weighting μ based on the month within which it falls, ranging linearly from 1 (October, when the termini are typically most retreated), to -1 (April, when the termini are typically most advanced). The mean weighting for each year, μ_a, thus provides an indication of the extent by which the available data points likely over or under estimate the true mean annual terminus position. For example, the only two data points for 1995 at DJ fall in August and September (when the glacier length will be close to its annual minimum). This gives μ_a = 0.5, and P is thus increased by 0.25 x r (= 0.3 km) with respect to P_{mean} to better approximate the true annual average terminus position. The difference between P_{mean} and P is shown in Figure 3 (being too small to plot in Figure 2g-h) and is in most cases negligible.

Statistics

Statistical comparison of T_A, Q, T_0, M_1 and M_2 with P is undertaken at the level of mean annual values. In Figure 5 (and Table S4) we consider data grouped from across the study glaciers, while in Figures 3 and 4 (and Table S3) we relate individual glacier-specific time series of anomalies in T_A, Q, T_0, M_1 and M_2 to those in P. Because these individual time series are in general non-stationary, classical linear regression may indicate a statistically significant correlation between

Glacier	*r* (km)
M3	0.42
T1	0.67
AB	0.57
HG	2.01
KG	2.93
BG	0.52
BG	0.42
DJ	1.17
WG	1.00
HK	0.09

Table S2. Mean annual range, *r*, in terminus position for each of the sample glaciers over the period 2010-2013.

variables in instances where in fact no relationship exists (Granger and Newbold, 1974). To reduce the risk of incorrectly interpreting such spurious relationships, we test for cointegration of the time series (Engle and Granger, 1987), a technique that has proven valuable in examining the relationships between non-stationary climate variables (e.g. Kaufmann and Stern, 2002, Mills, 2009, Beenstock et al., 2012). Cointegration occurs when a relationship between two or more non-stationary time series produces residuals that are themselves stationary, indicating a functional relationship that remains constant in time. A more thorough description of this approach, and its application in climate science, is provided by Kaufman and Stern (2002). We perform an Engle-Granger test for cointegration on each of the combinations of forcing and response time series using the *egcitest* function in Matlab R2016a (www.mathworks.com). Where linear regression indicates a significant correlation but cointegration is not established (at $p < 0.05$), we recognise the increased risk that this correlation may be spurious. All R^2 values given throughout the paper are significant at $p < 0.05$, with the specific p value given in each case, and all statistical values provided in Tables S3-4.

Glacier		T_A'				Q'				T_0'			
	n	***a*** [km / °C]	R^2	***p*** (correlation)	***p*** (cointegration)	***a*** [km / ($m^3 s^{-1}$)]	R^2	***p*** (correlation)	***p*** (cointegration)	***a*** [km / °C]	R^2	***p*** (correlation)	***p*** (cointegration)
M3	17	-2.138	0.46	<0.01	0.04	-0.209	0.60	<0.01	0.01	-4.679	0.61	<0.01	0.04
T1	17	-0.716	(0.39)	<0.01	0.10	-0.090	0.59	<0.01	0.03	-2.164	(0.36)	<0.01	0.15
AB	16	-1.641	0.51	<0.01	0.05	-0.139	0.63	<0.01	0.05	-4.127	0.73	<0.01	0.03
HG	20	-1.745	0.43	<0.01	0.03	-0.112	0.75	<0.01	<0.01	-4.977	0.74	<0.01	<0.01
KG	20	-1.388	(0.24)	0.03	0.11	-0.052	0.58	<0.01	<0.01	-2.249	(0.47)	<0.01	0.31
BG	17	-	-	<0.01	0.50	-0.111	(0.45)	<0.01	0.10	-	-	0.47	0.81
VG	17	-	-	0.16	0.03	-	-	0.09	0.02	-	-	0.68	<0.01
DJ	20	-0.124	0.36	<0.01	<0.01	-0.007	0.37	<0.01	<0.01	-0.338	0.39	<0.01	<0.01
WG	17	-	-	0.08	0.01	-	-	0.06	0.05	-	-	0.14	0.24
HK	17	-0.237	(0.38)	<0.01	0.37	-0.090	(0.34)	0.01	0.45	-0.740	(0.55)	<0.01	0.07
*All south**	90	n/a	0.52	<0.01	0.03	n/a	0.73	<0.01	<0.01	n/a	0.71	<0.01	0.03
*All north**	88	n/a	(0.53)	<0.01	0.08	n/a	(0.59)	<0.01	0.09	n/a	(0.51)	<0.01	0.06

158

Glacier		M_1'				M_2'			
	n	***a*** [km / ($m^3 s^{-1}$ °C)]	R^2	***p*** (correlation)	***p*** (cointegration)	***a*** [km / ($m\ s^{-1/3}$ °C)]	R^2	***p*** (correlation)	***p*** (cointegration)
M3	17	-0.030	0.62	<0.01	0.01	-0.579	(0.43)	<0.01	0.05
T1	17	-0.012	0.59	<0.01	0.03	-0.288	(0.36)	<0.01	0.11
AB	16	-0.020	0.65	<0.01	0.04	-0.596	0.58	<0.01	0.03
HG	20	-0.020	0.76	<0.01	<0.01	-0.828	0.70	<0.01	0.01
KG	20	-0.012	0.59	<0.01	0.03	-0.697	(0.46)	<0.01	0.20
BG	17	-0.025	(0.29)	0.02	0.39	-	-	0.10	0.68
VG	17	-	-	0.16	0.01	-	-	0.21	0.01
DJ	20	-0.002	0.44	<0.01	<0.01	-0.119	0.46	<0.01	<0.01
WG	17	-0.001	0.32	0.02	0.03	-0.054	0.25	0.04	0.05
HK	17	-0.029	(0.41)	<0.01	0.46	-0.403	(0.44)	<0.01	0.43
*All south**	90	n/a	0.75	<0.01	<0.01	n/a	0.63	<0.01	0.03
*All north**	88	n/a	0.63	<0.01	0.03	n/a	(0.55)	<0.01	0.05

159

160 Table S3. Coefficient *a* and R^2 values for the relationship $P' = aF'$, where P' is glacier terminus position anomaly and F' is forcing anomaly (i.e. T_A', Q', T_0',
161 M_1' or M_2'), expressed relative to the 1993-2012 mean. Missing values are not significantly correlated at $p < 0.05$, while values in brackets indicate that
162 time series are not significantly cointegrated at $p < 0.05$ (Methods). R^2 values for the 'All north' and 'All south' subsets (*) are given for consistency
163 with Figures 3 and 4 – note that because these are only applicable to the combined normalised data sets ($\tilde{T}_A$ $\tilde{Q}$, $\tilde{T}_0$, $\tilde{M}_1$ and $\tilde{M}_2$) as shown in Figure 3f
164 and l, values of *a* are not given. Also shown in each case is the sample size *n*.

165

Dataset	*n*	T_A			Q			T_0			M_1			M_2		
		a [km / ℃]	R^2	***p***	***a*** [km / ($m^3 s^{-1}$)]	R^2	***p***	***a*** [km / ℃]	R^2	***p***	***a*** [km / $m^3 s^{-1}$ ℃]	R^2	***p***	***a*** [km / $m\ s^{-1/3}$ ℃]	R^2	***p***
All glaciers (P')	178	-0.802±0.230	0.21	<0.01	-0.059±0.011	0.41	<0.01	-2.110±0.418	0.36	<0.01	-0.014±0.002	0.54	< 0.01	-0.541±0.0896	0.44	<0.01
All glaciers (ΔP)	10	-	-	0.47	-	-	0.12	-2.906±1.25	0.41	0.01	-0.018±0.006	0.54	0.01	-0.628±0.221	0.57	0.01

Table S4. Coefficient *a* (including 95 % confidence intervals) and R^2 values for the relationship between terminus position and the environmental forcings for the combined 'All glaciers' datasets. The upper row shows the relationship $P' = aF'$, where P' and F' represent the anomalies (relative to the 20-year mean) in terminus position and the forcings (i.e. T_A', Q', T_0', M_1' and M_2') respectively (Figure 5a-e). The lower row shows the relationship $\Delta P = a\,\Delta F$, where ΔP and ΔF represent the overall change (2010-2012 mean minus the 1993-1995 mean) in terminus position and forcings (i.e. ΔT_A, ΔQ, ΔT_0, ΔM_1 and ΔM_2) respectively (Figure 5f-j). Also shown in each case is the sample size *n* and *p* value. Missing values are not significant at $p < 0.05$

References

Azetsu-Scott, K. and Syvitski, J. P. M. (1999) 'Influence of melting icebergs on distribution, characteristics and transport of marine particles in an East Greenland fjord', *Journal of Geophysical Research-Oceans,* 104(C3), pp. 5321-5328.

Bamber, J. L., Griggs, J. A., Hurkmans, R. T. W. L., Dowdeswell, J. A., Gogineni, S. P., Howat, I., Mouginot, J., Paden, J., Palmer, S., Rignot, E. and Steinhage, D. (2013) 'A new bed elevation dataset for Greenland', *Cryosphere,* 7(2), pp. 499-510.

Beenstock, M., Reingewertz, Y. and Paldor, N. (2012) 'Polynomial cointegration tests of anthropogenic impact on global warming', *Earth System Dynamics,* 3(2), pp. 173-188.

Bevan, S. L., Luckman, A. J. and Murray, T. (2012) 'Glacier dynamics over the last quarter of a century at Helheim, Kangerdlugssuaq and 14 other major Greenland outlet glaciers', *Cryosphere,* 6(5), pp. 923-937.

Cowton, T., Sole, A., Nienow, P., Slater, D., Wilton, D. and Hanna, E. (2016) 'Controls on the transport of oceanic heat to Kangerdlugssuaq Glacier, east Greenland', *Journal of Glaciology*.

Dee, D. P., Uppala, S., Simmons, A., Berrisford, P., Poli, P., Kobayashi, S., Andrae, U., Balmaseda, M., Balsamo, G. and Bauer, d. P. (2011) 'The ERA-Interim reanalysis: Configuration and performance of the data assimilation system', *Quarterly Journal of the royal meteorological society,* 137(656), pp. 553-597.

Dowdeswell, J. (2004) *Cruise report - JR106b. RSS James Clark Ross. NERC Autosub Under Ice thematic programme. Kangerdlugssuaq Fjord and shelf, east Greenland*.

Engle, R. F. and Granger, C. W. J. (1987) 'Cointegration and error correction - representation, estimation and testing', *Econometrica,* 55(2), pp. 251-276.

Fenty, I., Willis, J. K., Khazendar, A., Dinardo, S., Forsberg, R., Fukumori, I., Holland, D., Jakobsson, M., Moller, D. and Morison, J. (2016) 'Oceans Melting Greenland: Early Results from NASA's Ocean-Ice Mission in Greenland', *Oceanography*.

Ferry, N., Parent, L., Garric, G., Drevillon, M., Desportes, C., Bricaud, C. and Hernandez, F. (2012) *Scientific Validation Report (ScVR) for Reprocessed Analysis and Reanalysis. MyOcean project report, MYO-WP04-ScCV-rea-MERCATOR-V1.0*.

Granger, C. W. and Newbold, P. (1974) 'Spurious regressions in econometrics', *Journal of econometrics,* 2(2), pp. 111-120.

Holfort, J., Hansen, E., Østerhus, S., Dye, S., Jonsson, S., Meincke, J., Mortensen, J. and Meredith, M. (2008) 'Freshwater fluxes east of Greenland', *Arctic-Subarctic Ocean Fluxes Defining the Role of the Northern Seas in Climate.,* 304.

Inall, M. E., Murray, T., Cottier, F. R., Scharrer, K., Boyd, T. J., Heywood, K. J. and Bevan, S. L. (2014a) 'Oceanic heat delivery via Kangerdlugssuaq Fjord to the south-east Greenland ice sheet', *Journal of Geophysical Research-Oceans,* 119(2), pp. 631-645.

Inall, M. E., Murray, T., Cottier, F. R., Scharrer, K., Boyd, T. J., Heywood, K. J. and Bevan, S. L. (2014b) 'Oceanic heat delivery via Kangerdlugssuaq Fjord to the south-east Greenland ice sheet', *Journal of Geophysical Research: Oceans*, 119(2), pp. 631-645. Available at: http://onlinelibrary.wiley.com/doi/10.1002/2013JC009295/abstract (Accessed 01).

Joughin, I., Smith, B. E., Howat, I. M. and Scambos, T. (2010a) 'MEaSUREs Greenland Ice Velocity Map from InSAR Data'. Available at: <Go to ISI>://WOS:000280930000005 (Accessed.

Joughin, I., Smith, B. E., Howat, I. M., Scambos, T. and Moon, T. (2010b) 'Greenland flow variability from ice-sheet-wide velocity mapping', *Journal of Glaciology,* 56(197), pp. 415-430.

Kaufmann, R. K. and Stern, D. I. (2002) 'Cointegration analysis of hemispheric temperature relations', *Journal of Geophysical Research-Atmospheres,* 107(D1-D2).

Lea, J. M., Mair, D. W. F. and Rea, B. R. (2014) 'Instruments and Methods Evaluation of existing and new methods of tracking glacier terminus change', *Journal of Glaciology,* 60(220), pp. 323-332.

Mills, T. C. (2009) 'How robust is the long-run relationship between temperature and radiative forcing?', *Climatic change,* 94(3-4), pp. 351.

Murray, T., Scharrer, K., James, T. D., Dye, S. R., Hanna, E., Booth, A. D., Selmes, N., Luckman, A., Hughes, A. L. C., Cook, S. and Huybrechts, P. (2010) 'Ocean regulation hypothesis for glacier dynamics in southeast Greenland and implications for ice sheet mass changes', *Journal of Geophysical Research-Earth Surface,* 115.

Seale, A., Christoffersen, P., Mugford, R. I. and O'Leary, M. (2011) 'Ocean forcing of the Greenland Ice Sheet: Calving fronts and patterns of retreat identified by automatic satellite monitoring of eastern outlet glaciers', *Journal of Geophysical Research-Earth Surface,* 116.

Shreve, R. L. (1972) 'Movement of water in glaciers', *Journal of Glaciology,* 11, pp. 205-214.

Straneo, F., Hamilton, G. S., Stearns, L. A. and Sutherland, D. A. (2016) 'Connecting the Greenland Ice Sheet and the Ocean: A case study of Helheim Glacier and Sermilik Fjord', *Oceanography,* 29(4), pp. 34-45.

Straneo, F. and Heimbach, P. (2013) 'North Atlantic warming and the retreat of Greenland's outlet glaciers', *Nature,* 504(7478), pp. 36-43.

Straneo, F., Sutherland, D. A., Holland, D., Gladish, C., Hamilton, G. S., Johnson, H. L., Rignot, E., Xu, Y. and Koppes, M. (2012) 'Characteristics of ocean waters reaching Greenland's glaciers', *Annals of Glaciology,* 53(60), pp. 202-210.

Wilson, N., Straneo, F. and Heimbach, P. (2017) 'Satellite-derived submarine melt rates and mass balance (2011–2015) for Greenland's largest remaining ice tongues', *The Cryosphere,* 11(6), pp. 2773-2782.

Wilson, N. J. and Straneo, F. (2015) 'Water exchange between the continental shelf and the cavity beneath Nioghalvfjerdsbrae (79 North Glacier)', *Geophysical Research Letters,* 42(18), pp. 7648-7654.

Wilton, D. J., Jowett, A. M. Y., Hanna, E., Bigg, G. R., Van Den Broeke, M. R., Fettweis, X. and Huybrechts, P. (2017) 'High resolution (1 km) positive degree-day modelling of Greenland ice sheet surface mass balance, 1870–2012 using reanalysis data', *Journal of Glaciology,* 63(237), pp. 176-193.